

ChemistryOpen

Supporting Information

Avoiding Pitfalls in Comparison of Activity and Selectivity of Solid Catalysts for Electrochemical HMF Oxidation

Sebastian Wöllner, Timothy Nowak, Gui-Rong Zhang, Nils Rockstroh, Hanadi Ghanem, Stefan Rosiwal, Angelika Brückner, and Bastian J. M. Etzold*

Supporting Information

Experimental Section

The cell for the three electrode setup is self-constructed by the TU Darmstadt mechanics workshop and can be used undivided or divided (Figure S1), wherefore a glass frit from *Lenz*[®] *Laborglass* with 10 mm diameter, 2.5 mm thickness and 4 μm pore size is placed between the left and right compartment to divide the working electrode (WE) from the plated platinum counter electrode (CE, *IKA*[®]). 0.01, 0.1 1 or 3 M KOH (*Acros Organics*, 85 %) is used as the electrolyte in this setup, while the reference electrode (RE) is Hg/HgO (*ALS Japan RE-61AP*). The potentiostat used in these measurements was a *Parstat*[®] *Multichannel* with PMC-1000 channels from *Ametek*[®] using the software *VersaStudio* to process all data.

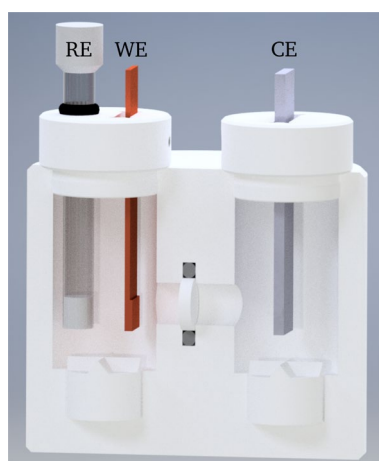


Figure S1: Cell setup with working electrode (brown, WE), reference electrode (blank, RE) in one compartment and counter electrode (grey, CE) in the other. Compartments can be divided by a glass frit (white disk).

The counter electrode material can influence the performance of the investigated catalyst system by hindering the complete electron cycle by *e.g.*, sluggish electron transfer. In case of HMF oxidation, the counter electrode reaction is the hydrogen evolution reaction (HER). As platinum is one of the best HER catalysts in alkaline media published^[1] that is also easily available, a platinum plate counter electrode is used in this work.

The electrode materials used are copper-sheet (Cu-sheet), graphite foil (*Sigraflex*[®]) and boron doped diamond (BDD) on titanium, the latter one synthesized^[2] and provided by the *WTM Nürnberg-Erlangen*. The catalysts are CuCoO_P, Nickel (Ni) and self-prepared copper-foam (Cu-foam). Cu-foam is prepared by using a Cu-sheet (overall dimension of 50 x 8 x 1 mm) as cathode and stainless steel mesh (*Beisser Metall*[®]) as anode in a 0.2 M CuSO₄ (*Fisher chemicals*, > 98 %) and 1.5 M H₂SO₄ (*Acros Organics*, 96 %) containing aqueous deposition solution. As a standard procedure, a current density of 3 A cm⁻² is applied until a charge of 10 C passed, which results in a foam thickness of 8 μm according to Shin and

Liu^[3]. The standard geometric area of the foam is about 0.5 cm², whereby the whole area is covered with foam, so no sheet is visible anymore and therefore not directly in contact with any electrolyte. Ni is prepared similarly to Cu-foam: Stainless steel mesh was also used as anode, and the main difference is the deposition onto BDD. Also, the deposition solution contains 75 mM NiSO₄ · 6 H₂O (*Acros Organics*, > 98 %) and just 5 C of charge were passed at a current density of 3 A cm⁻².

CuCoO_P is synthesized in a two step synthesis following two literature protocols. At first, the nitrates of Cu and Co are dissolved in a mixture of water and citric acid and stirred at room temperature.^[4] After gelation at 90 °C and drying at 120 °C, the samples are calcined at 300 °C in air to get the bimetallic oxide CuCoO (atomic ratio of Cu:Co = 6:1), which was synthesized and provided by the *LIKAT* in Rostock.^[4] Afterwards, the sample was thoroughly grounded with NaPO₂H₂ · H₂O (*Acros Organics*, > 99 %) before placing it in a tubular furnace (SR 70-200/12 *Carbolite*[®] Gero 30-3000 °C tubular furnace with a X0004516/-V2 *QCS* quartz glass tube (length: 900 mm, diameter: 46 mm)) at 300 °C for 2 hours under N₂ gas flow.^[5] The sample was then washed with water, centrifuged and dried in a vacuum furnace at 80 °C to get the phosphor treated bimetallic system CuCoO_P.^[5]

Scanning transmission electron microscopy (STEM) micrographs were obtained on a probe aberration-corrected JEM-ARM200F (Jeol, Corrector: CEOS) at 200 kV. The chemical composition was analyzed by an attached JED-2300 (Jeol) energy dispersive X-ray spectrometer (EDXS). Sampling was done by dry deposition of the catalyst powder without any pretreatment on a holey carbon supported Ni grid (mesh 300), which was then transferred to the microscope.

CuCoO_P is an amorphous material and its consistency as well as instability under the electron beam complicated its investigation in the transmission electron microscope. While copper was not found in the investigated regions, cobalt, oxygen, phosphorous and also sodium have been observed in the corresponding EDX spectra. The presence of sodium can be explained by the use of sodium hypophosphite (NaPO₂H₂) in the phosphorous treating step. A brief overview can be seen in Figure S2.

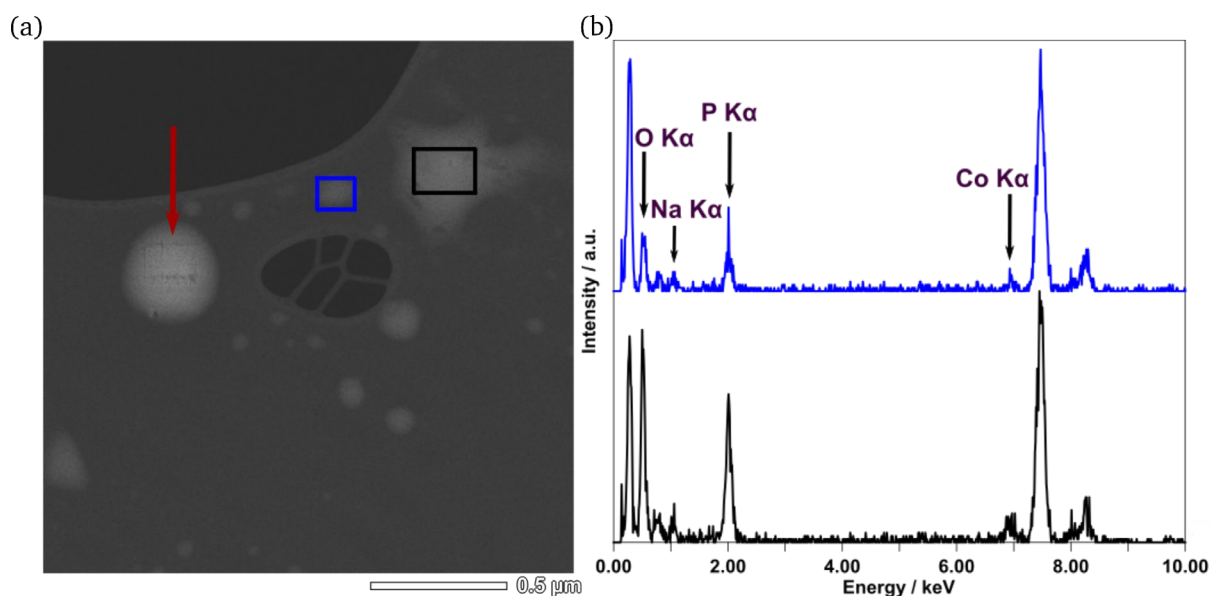


Figure S2: STEM-HAADF image of CuCoO_P (a) and EDX spectra of the highlighted areas (b). The red arrow in the left image indicates damage of the sample by the electron beam during the EDX measurement. In the EDX spectra, oxygen, sodium, phosphorous, and cobalt have been found, but no copper has been observed.

An inVia Raman microscope (Renishaw) equipped with a 633 nm Laser and a power between 0.161 and 1.61 mW was applied to collect the Raman spectra. The samples were mounted onto object slides and an objective with a 50fold magnification was used. To examine the homo/heterogeneity of the material, spectra were collected at different positions on the sample.

Raman spectroscopy was intended to provide insight into the species present in CuCoO_P. Due to the heterogeneity of the material, spectra were evaluated at different positions of the catalyst (Figure S3). The blue graph clearly shows the D and G band of carbon at 1335 and 1581 cm^{-1} , respectively^[6], that stem from adventitious carbon species present in the material. Also, the spectra excludes any phosphite (HPO_3^{2-}) or hypophosphite (H_2PO_2^-) species being present, because their mode ($\sim 1000 \text{ cm}^{-1}$) is not detectable.^[7] Copper oxide species can be excluded in the catalyst since signals for Cu_2O (218, 523 and 623 cm^{-1}), CuO (298, 347, 490 cm^{-1}) and $\text{Cu}^{\text{III}}\text{O}_x$ (603 cm^{-1}) are missing.^[8] Also, signals for $\text{Cu}(\text{OH})_2$ (293 and 485 cm^{-1}) are not detected in the Raman spectra.^[8] Cobalt oxide species like CoOOH (503 and 635 cm^{-1})^[9] and Co_3O_4 (480, 520 618 and 688 cm^{-1})^[10] can be ruled out as well since their bands are not present in the spectra. All of these missing oxide species imply a successful phosphorous treatment with phosphorous replacing oxygen in the catalyst. However, signals for metal phosphides are also not detected. Neither $\text{CuP}^{[11]}$ nor $\text{Cu}_{3-x}\text{P}^{[12]}$ nor $\text{Co}_2\text{P}^{[13]}$ which show Raman bands in a range of 0 to 2000 cm^{-1} are present. Potentially, phosphonate species might be present, but based on the present results this is unclear so far.

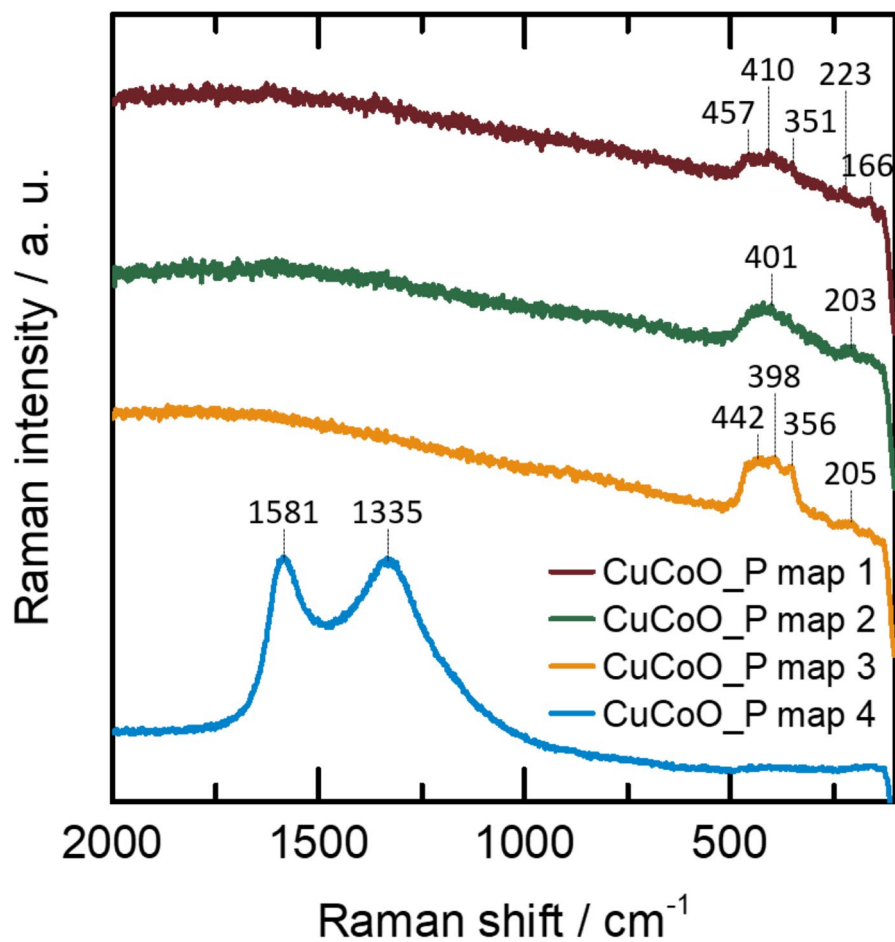


Figure S3: Raman spectra of the phosphor treated bimetallic system CuCoO_P. Red, green blue: Raman spectra of different spots of CuCoO_P (CuCoO_P map 1-3). Pink: Raman spectra of the carbon support of CuCoO_P.

Influence of Separator

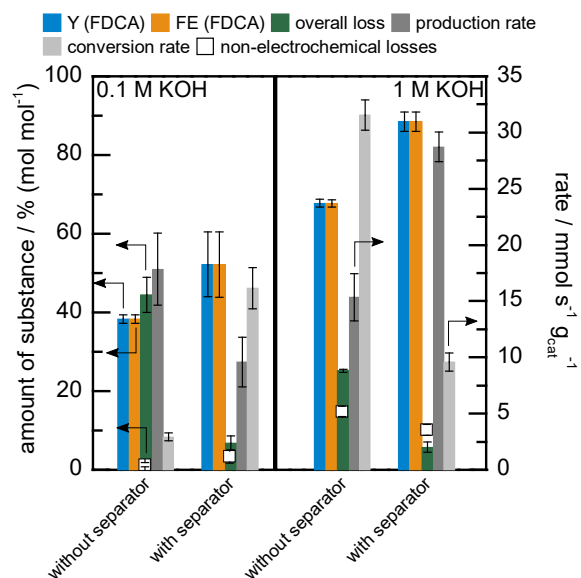


Figure S4: Yield and faradaic efficiency towards FDCA (Y (FDCA) (blue) and FE (FDCA) (orange), respectively), overall loss (green) non-electrochemical loss for comparison (blank squares), as well as production and conversion rate (dark and light grey, respectively) for electrolysis of 5 mM HMF in 0.1 (left compartment) and 1 M KOH (right compartment) in a setup with and without separator at 30 °C. Cu-foam was used as anode electrode and platinum as cathode electrode.

HPLC

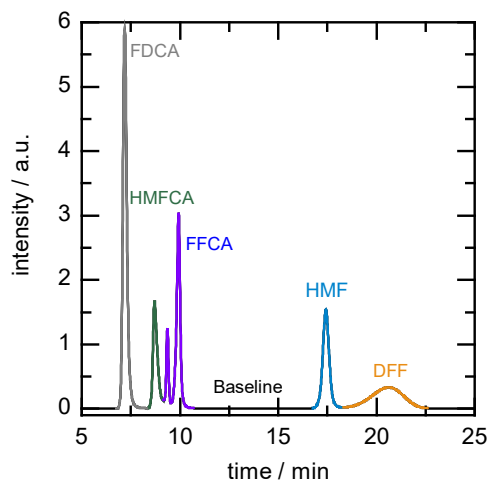


Figure S5: Extracted chromatogram of HPLC with every detected reactant. HMF (17.5 minutes), DFF (21 minutes), HMFCFA (8.5 minutes), FFCA (10 minutes), FDCA (7 minutes).

- [1] H. Yin, S. Zhao, K. Zhao, A. Muqsit, H. Tang, L. Chang, H. Zhao, Y. Gao, Z. Tang, *Nature Communications* **2015**, *6*, 1-8.
- [2] B. Schorr, H. Ghanem, S. Rosiwal, W. Geissdorfer, A. Burkovski, *World Journal of Microbiology and Biotechnology* **2019**, *35*, 48.
- [3] H.-C. L. Shin, Meilin, *Chemistry of Materials* **2004**, *16*, 5460 - 5464.
- [4] M. Polyakov, A.-E. Surkus, A. Maljus, S. Hoch, A. Martin, *ChemElectroChem* **2017**, *4*, 2109-2116.
- [5] B. You, N. Jiang, M. Sheng, S. Gul, J. Yano, Y. Sun, *Chemistry of Materials* **2015**, *27*, 7636-7642.
- [6] N. Larouche, B. L. Stansfield, *Carbon* **2010**, *48*, 620-629.
- [7] R. I. Bickley, H. G. M. Edwards, A. Knowles, J. K. F. Tait, R. E. Gustar, D. Mihara, S. J. Rose, *Spectrochimica Acta* **1994**, *50A*, 1277-1285.
- [8] Y. Deng, A. D. Handoko, Y. Du, S. Xi, B. S. Yeo, *ACS Catalysis* **2016**, *6*, 2473-2481.
- [9] T. Pauporté, L. Mendoza, M. Cassir, M. Bernard, J. Chivot, *Journal of the Electrochemical Society* **2004**, *152*, C49.
- [10] L. Mendoza, R. Baddour-Hadjean, M. Cassir, J. P. Pereira-Ramos, *Applied Surface Science* **2004**, *225*, 356-361.
- [11] C. C. Hou, Q. Q. Chen, C. J. Wang, F. Liang, Z. Lin, W. F. Fu, Y. Chen, *ACS Applied Material Interfaces* **2016**, *8*, 23037-23048.
- [12] L. De Trizio, R. Gaspari, G. Bertoni, I. Kriegel, L. Moretti, F. Scotognella, L. Maserati, Y. Zhang, G. C. Messina, M. Prato, S. Marras, A. Cavalli, L. Manna, *Chemistry of Materials* **2015**, *27*, 1120-1128.
- [13] H. Li, Q. Li, P. Wen, T. B. Williams, S. Adhikari, C. Dun, C. Lu, D. Itanze, L. Jiang, D. L. Carroll, G. L. Donati, P. M. Lundin, Y. Qiu, S. M. Geyer, *Advanced Materials* **2018**, *30*, 1705796.